Hippocampal Subfield Segmentation Protocol at 4T

John Pluta, Susanne Mueller, Caryne Craige & Paul Yushkevich

Contact: jpluta@mail.med.upenn.edu

Contents:

Segmenting the hippocampus:

1. Basic hippocampal anatomy

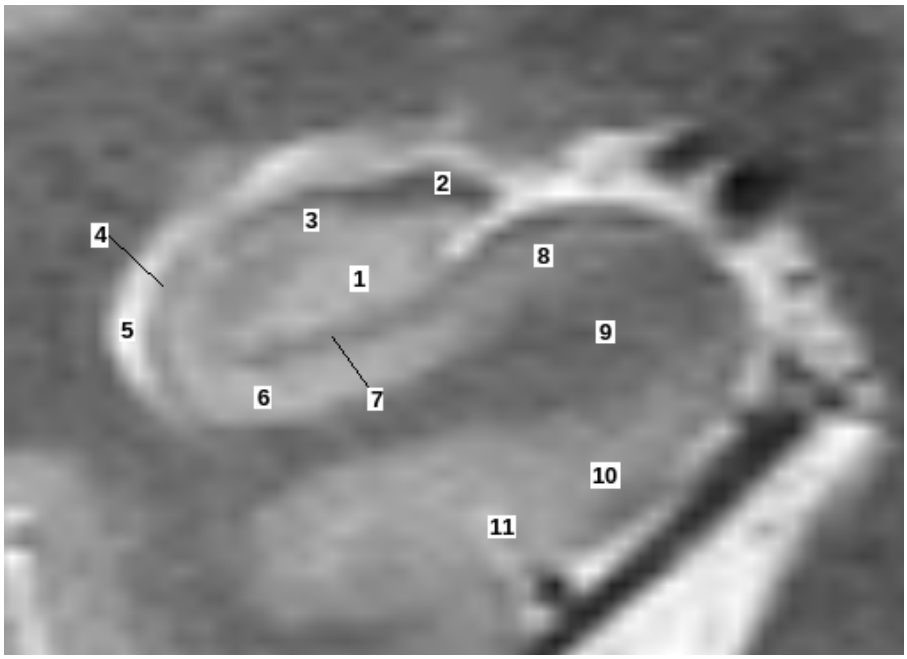

Fig. 1.1: Typical coronal slice of the hippocampal body. (1) Dentate gyrus (DG), (2) fimbria, (3) CA2/CA3, (4) alveus, (5) lateral ventricle, (6) CA1, (7) stratum structures (stratum moleculare, stratum lacunosum, stratum radiatum) (STR) , (8) subiculum, (9) temporal cortex, (10) entorhinal cortex (ERC), (11) collateral sulcus.

Hippocampal body slices most often appear in one of two shapes. The most common is in an ellipse, and most diagrams and atlases refer to this shape. Circular shaped body slices are less common but still encountered. All geometric boundary definitions should work as well with both shapes.

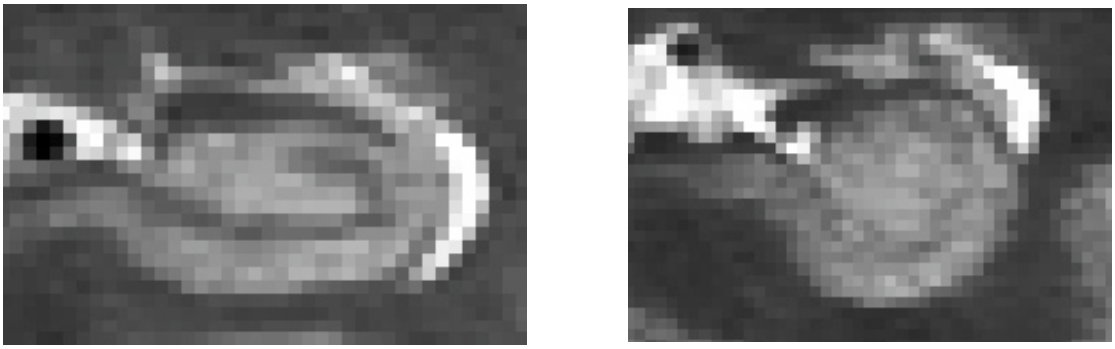

Fig. 1.2: Ellipse-shaped hippocampal body slice (left), circle-shaped body slice (right)

2. Information about the dataset

The images used in defining this protocol were acquired in [Mueller et al 2007]: a high resolution T2 weighted fast spin echo sequence (TR/TE: 3500/19 ms, echo train length 15, 18.6 ms echo spacing, 160 flip angle, 100% oversampling in ky direction, 0.4 x 0.4 mm in plane resolution, 2 mm slice thickness, 24 interleaved slices without gap.

3. Setting up SNAP

It is strongly recommended that you install the latest version of ITK-SNAP for subfield segmentation. Linear interpolation and the annotation tool are only available in v. 1.8.0 and above. SNAP is available at www.itksnap.org

Contrast

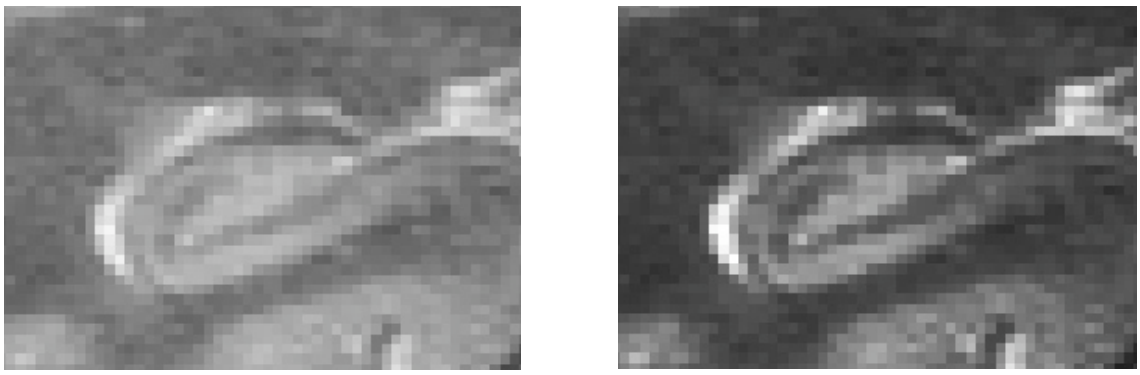

Fig. 3.1: Auto-contrast vs. contrast set manually to maximize appearance of STR

Contrast should be set to maximize the appearance of the hypointense line separating CA1 and DG (comprised of STR). To set contrast in SNAP:

Options -> Image Contrast

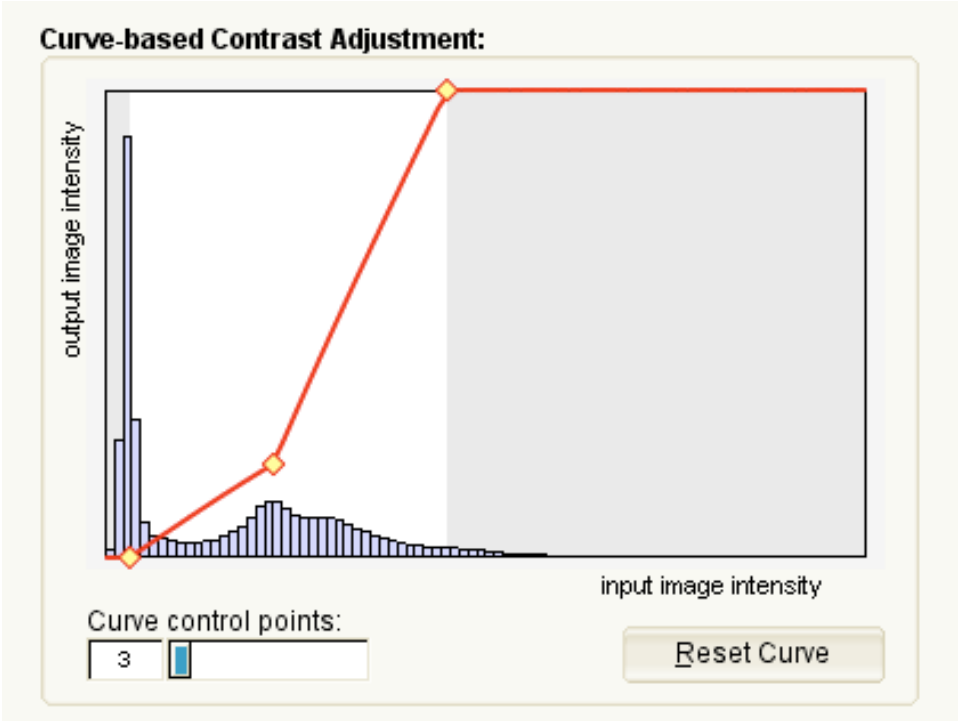

Fig. 3.2: Typical contrast settings, set to maximize the appearance of STR.

3D Rendering

Certain subfields are very small, sometimes only a few voxels per slice, meaning that any kind of smoothing can obscure errors that would otherwise be detected on the 3D rendering of the segmentation. For this reason, smoothing should be disabled.

Tools -> Display Options -> (uncheck) Gaussian Smoothing

Label Descriptions

The names and values assigned to each label should be kept consistent across raters, to simplify comparisons. Once the grayscale image is loaded, load the label description file "subfield_labels.txt":

Segmentation -> Load Label Descriptions -> subfield_labels.txt

Nearest-Neighbor vs. Linear Interpolation

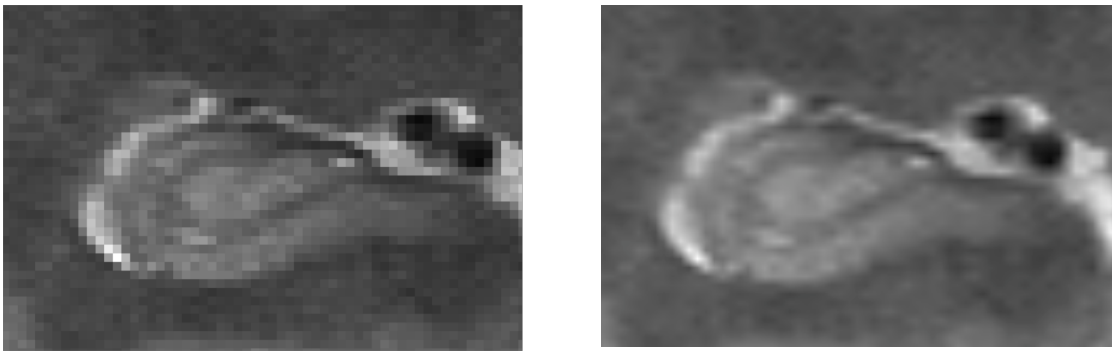

Fig. 3.3: Sample body slice displayed with nearest-neighbor interpolation (left) and linear interpolation (right)

By default, SNAP displays images using nearest-neighbor interpolation. However, it is subject to partial voluming effects that can obscure certain boundaries, particularly between CA1 and DG. In certain images, switching to linear interpolation can help to better define these boundaries.

To change views between linear and cubic interpolation:
Tools -> Display Options -> Layout -> Use Linear Interpolation

Annotation Tool

The annotation tool provided with SNAP is important in subfield labels as it provides as objective and accurate way to make the geometric determinations that the protocol suggests. Any step that requires the measurement of the length of a line, or the angle between two lines, should be completed using the annotation tool.

4. Qualitative Criteria

There is some degree of variability inherent in in-vivo image acquisition, and the degree of precision that subfield segmentation requires means that certain images will not be clear enough to be reliably segmented. Before beginning segmentation, scroll through the image and try to identify the common structures and how they will be segmented. All of the subfield segmentation boundaries described in this text are based on [Mueller et al, 2007] and [Duvernoy et al. 2005], as well as histology sections from [Thammaroj et al. 2005, Chakeres et al. 2008] and very high-resolution scans acquired at 9.4T [Yushkevich et al. 2009, Fatterpekar et al. 2002].

The dentate gyrus is the critical structure for subfield segmentation- if this cannot be reliably identified through most of the slices, segmentation is impossible. The subject may still be viable if DG is obscured on only one or two slices, if a reasonable approximation can be made based on the segmentation of the surrounding slices.

However this approach will certainly affect reproducibility, and should be used with caution.

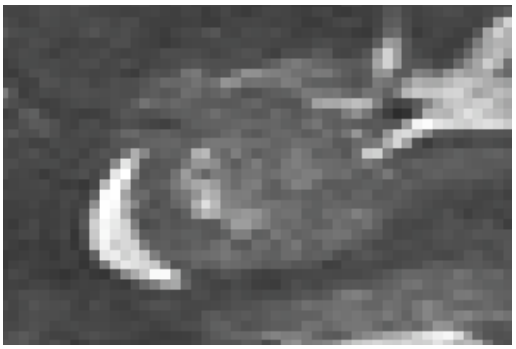

Fig. 4.1: Body slice with poor resolution and atypical anatomy.

Cysts, arteries, and imaging artifacts are all relatively common occurrences. In some cases, an abnormality can be large enough to cause a substantial deformity. Since some subfields are geometrically determined, extremely atypical subjects may have to be excluded.

5. Head

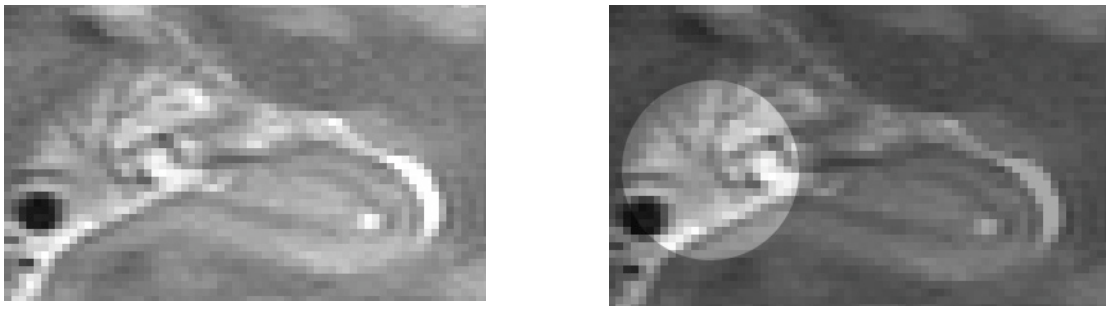

Fig. 5.1: Emergence of uncal apex

The head of the hippocampus is segmented as one label. It begins in the first slice in which the uncal apex is visible. Head slices should be segmented to the extent that they are still discernable in the image. In most subjects, this will be 6-7 slices beyond the slice containing the emergence of the uncal apex.

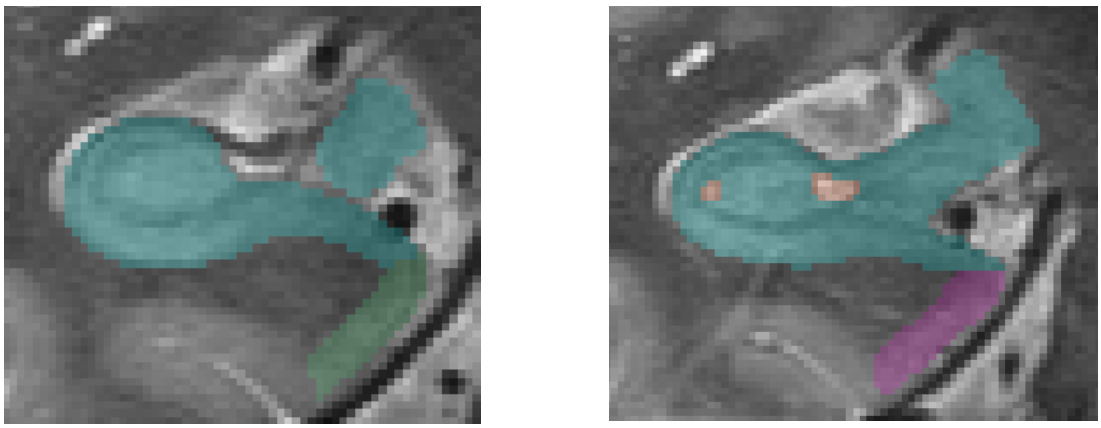

Fig 5.2: Two consecutive head slices. The beginning of the head is denoted by the emergence of the uncal apex.

Although subiculum is present in head slices, there is no way to reliably distinguish it from the hippocampal head, and it is included as part of this label. Hippocampal head should be segmented up to the most medial point of the gyrus (this is the same way the boundary of subiculum and PHG is determined), with the edge of this boundary being parallel to the outer edge of the head.

6. Body

Dentate Gyrus

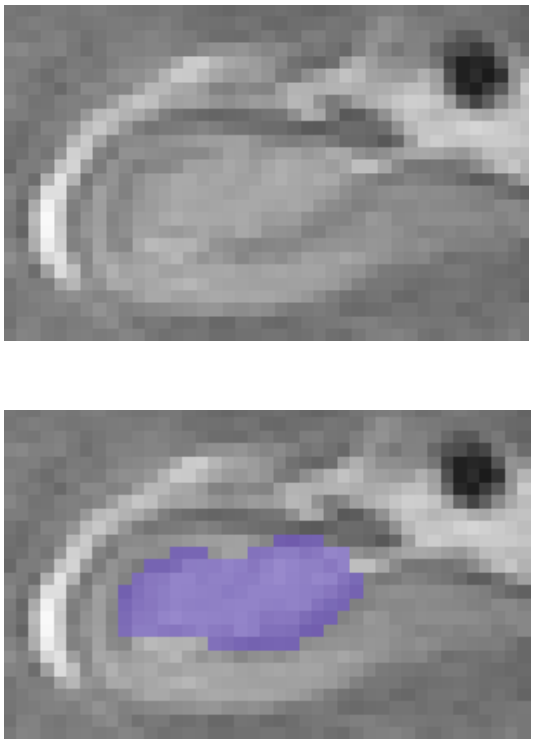

Fig. 6.1: Sample DG segmentation

Begin body sections by identifying the dentate gyrus. It is separable from the CA structures by the presence of the dark band around DG, and the vestigial hippocampal sulcus (VHS) in tail sections. This band is comprised of the stratum moleculare, lacunosum and radiatum. Switching to linear interpolation view can be helpful in identifying this border, particularly in images that are more affected by partial-volume averaging.

At this resolution, STR cannot be reliably segmented as a separate label, so these voxels should be included in DG and CA, dividing the dark band approximately between the two structures. In the superior portion of the slice, dark band should generally be assigned to DG, because this provides a closer estimate to the thickness of the CA subfields.

CA1

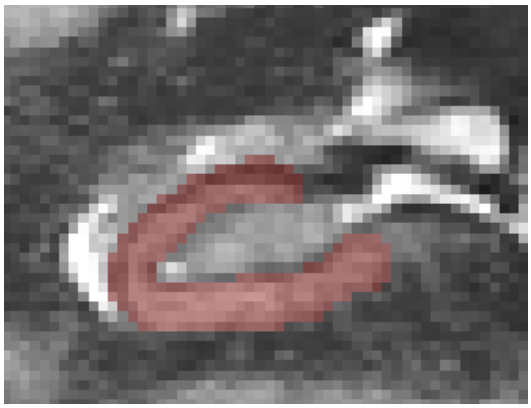

CA is the largest part of the hippocampal body. It wraps around DG, and the two are separated by STR. The fimbria is visible as the large, dark structure over DG. The alveus is a band of white matter that borders CA, and transforms into the fimbria. Alveus is typically only separable in high-quality images, so to ensure consistency it is included as part of CA. The transition between CA and DG is delineated by the fimbrio-dentate sulcus.

Fig. 6.2: Sample CA Segmentation

CA1/Subiculum/Entorhinal Cortex/Parahippocampal Gyrus

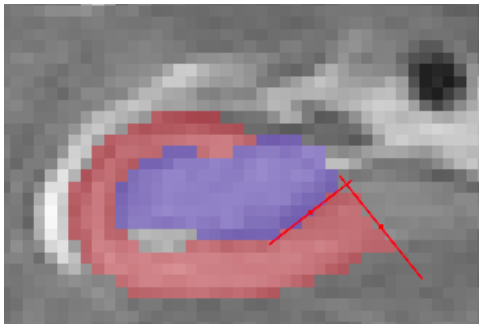

The boundary between CA1 and subiculum is measured by drawing a straight line along the edge of DG, and drawing a second line perpendicular to the first at the edge of the most medial, most superior voxel of DG. Note the presence of a hippocampal cyst, which is excluded from CA1.

Fig. 6.3: Sample CA1 and DG segmentation with CA1 boundary

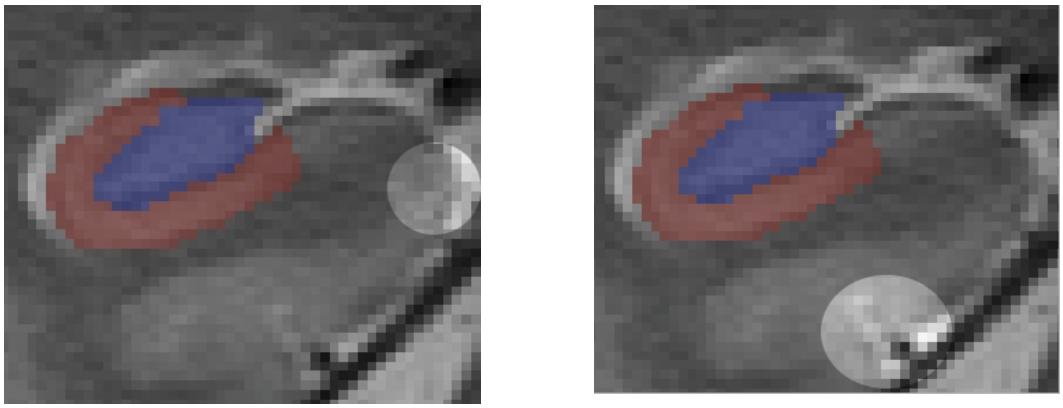

Fig. 6.4: Medial extent of temporal cortex (left), collateral sulcus (right)

Subiculum and ERC/PHG are defined between the edge of CA1 and the most medial point of the collateral sulcus. Thickness of these structures is determined by the thickness of CA1 at the point where it transitions to subiculum, and should be kept consistent throughout both structures. ERC/PHG is separated from subiculum by

locating the most medial point of the temporal cortex, and drawing a line parallel to the outer edge of CA1 (Fig. 6.6). Finally, the lateral boundary of ERC/PHG should be normal to the outer edge of CA1.

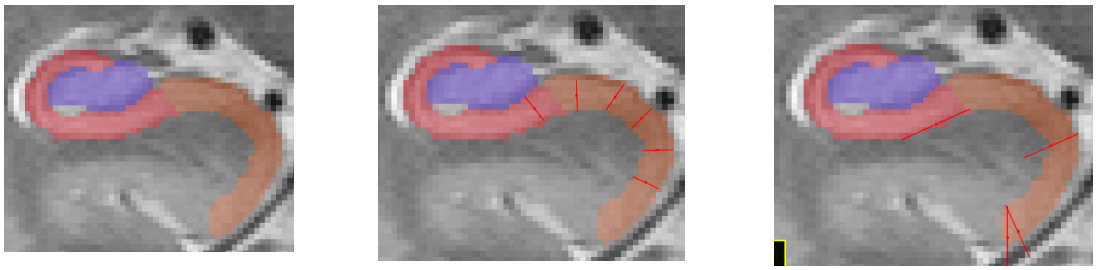

Fig. 6.5: Segmentation with subiculum added. The annotation tool can be used to ensure that the width stays consistent.

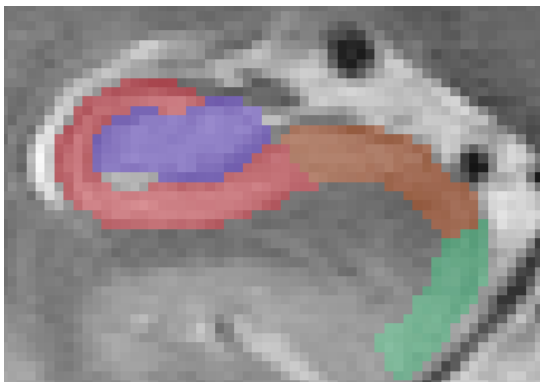

Fig 6.6: Hippocampus segmentation with DG, CA1, subiculum, and entorhinal cortex.

There are several variants of the collateral sulcus. The two most prominent types are the collateral sulcus pattern and the rhinal-collateral sulcus pattern (Zhan et al 2009). In the collateral pattern, the collateral sulcus appears between the lateral ventricle and the occipito-temporal sulcus, while in the rhinal pattern the collateral sulcus does not appear or is poorly defined. In rhinal pattern cases, the shallow rhinal sulcus should be used which becomes more prominent in anterior slices.

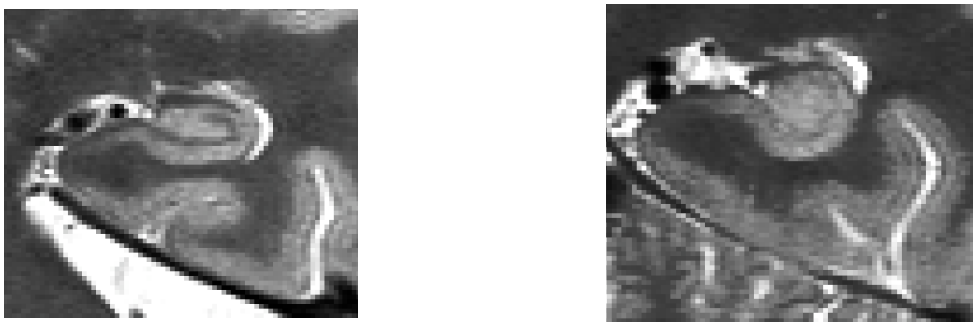

Fig. 6.7: Two most common patterns of the collateral sulcus: collateral (left) and rhinal pattern (right).

CA2/CA3

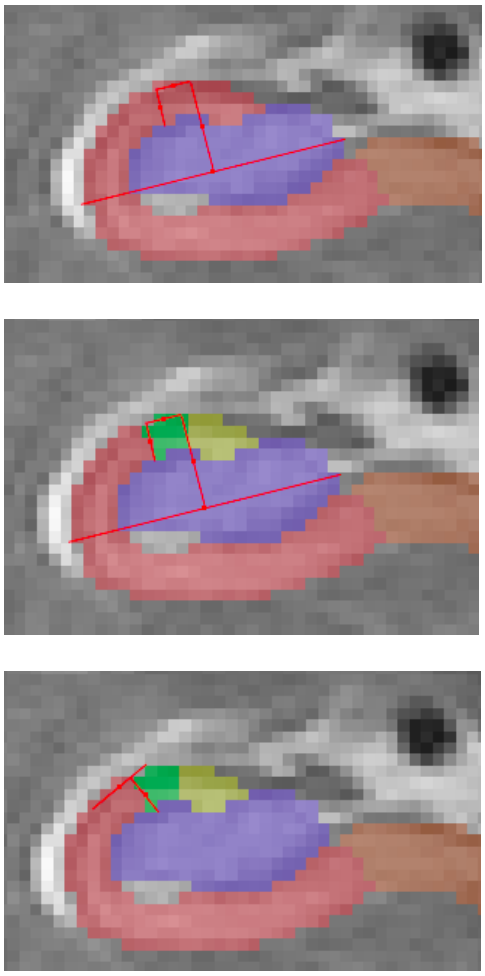

To segment CA2 and CA3, begin by using the annotation tool to draw a line across the longest length of the hippocampal body. This should extend from the end of the most medial point of DG to the furthest point on CA1, as measured across the longest distance of DG. From the midpoint of the first line, draw a second line perpendicular to the first that extends to the edge of CA1. This line separates CA2 from CA3.

The thickness of CA at this point is used to determine the width of the CA2 subfield. Measure the thickness using the annotation tool, and draw a line of that length from the edge of the second line (see Fig. 6.7). This determines the CA1/CA2 boundary. Finally, the CA1/CA2 boundary should be normal to the outer surface of CA, measured at the most lateral point of CA2.

Fig. 6.8: Delineation of CA2/CA3

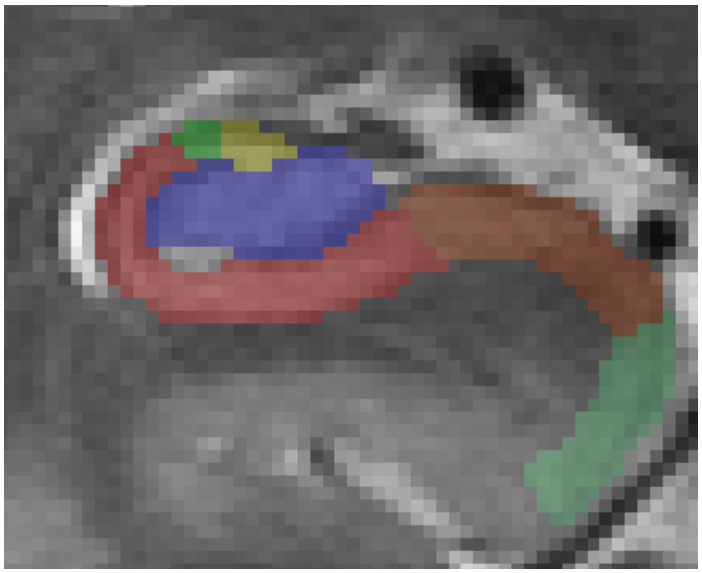

Fig. 6.9: Sample body slice with CA1, CA2, CA3, DG, subiculum, and ERC.

Miscellaneous Structures

Cysts commonly appear between DG and CA as hypo-intense regions separate from either structure. These are segmented under the MISC label and are generally not counted towards volume measurements.

If an area is ambiguous, check the surrounding slices and other views to determine what it is. Anything that is of markedly different intensity, or discontinuous from DG and CA1 is most likely a separate structure and should be segmented under MISC. Some of these structures are quite small, and due to the slice thickness, may only appear in a single slice.

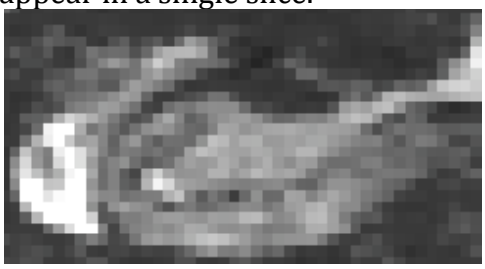

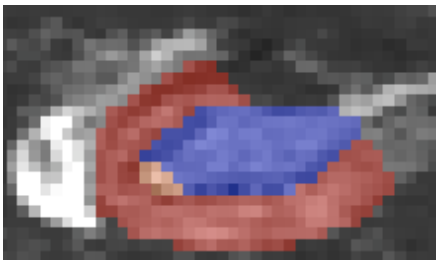

Fig. 6.91: Segmentation of a hippocampal cyst

7. Tail

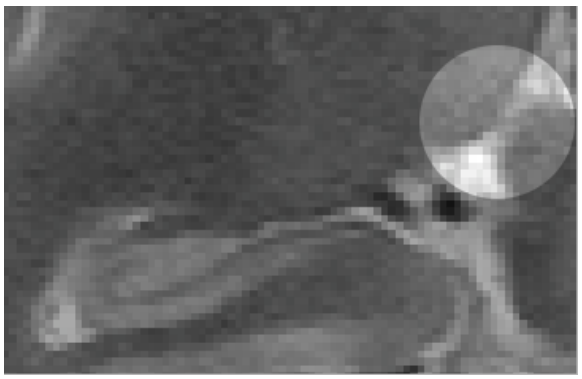

Fig. 7.1: Gradual joining of third ventricle and ambient cistern, over 2 consecutive slices.

Tail labeling begins in the first slice where the wing of the ambient cistern becomes visible. The wing of the ambient cistern is the small area of CSF separating the ambient cistern and the third ventricle. The slice immediately anterior to this is also labeled as tail, as well as the two slices posterior to the first.

This method may possibly exclude some part of the terminal section of the tail. However that boundary is ambiguous at this resolution, and marking would likely be inconsistent. The described boundary is easily found and captures a representative portion of the tail.

Subiculum/PHG in Tail Sections

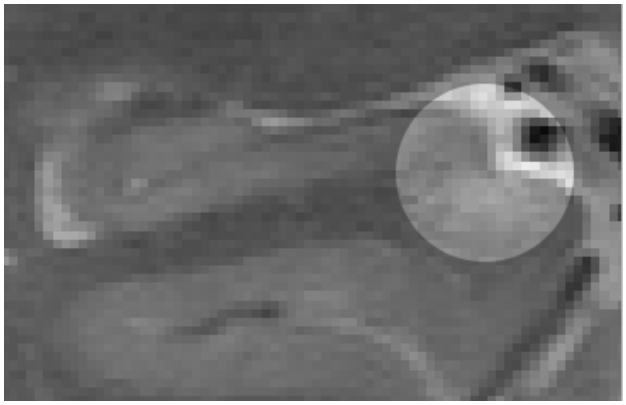

Subiculum and PHG are segmented in tail sections using the same boundary definitions as in body sections. Tail sections should include these subfields until the initial appearance of the anterior calcarine sulcus. This will be anywhere from 0 to a maximum of 2 slices.

Fig. 7.2: Anterior calcarine sulcus

8. 3D Rendering

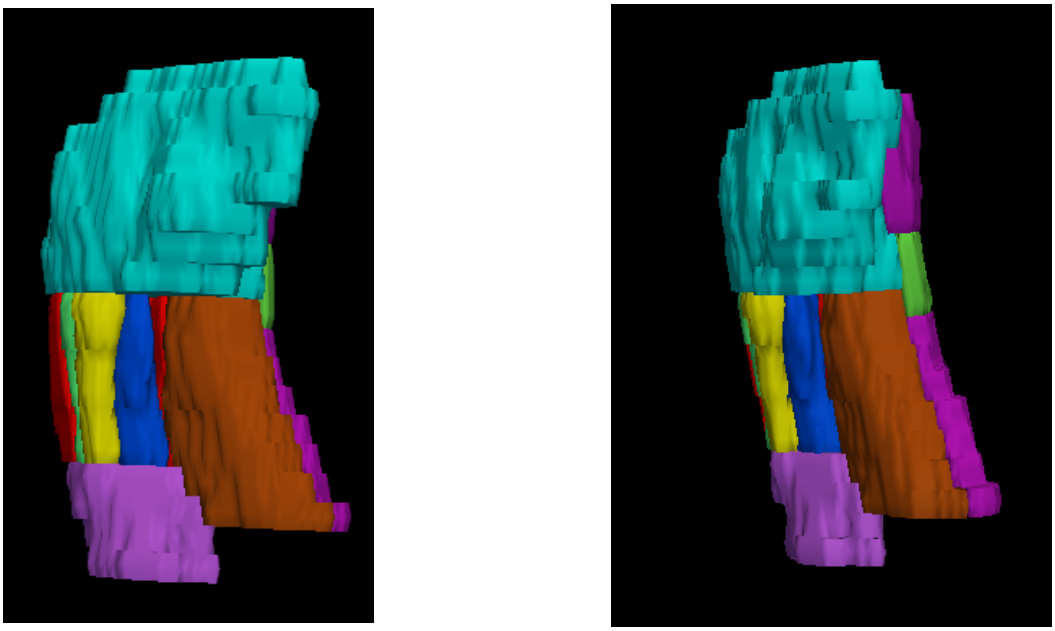

Fig. 8.1: 3-dimensional representation of hippocampus with head, DG, CA1, CA2, CA3, tail, subiculum, ERC, and PHG.

Rendering a segmentation in three dimensions can be helpful in creating consistent and anatomically correct model. Some errors that are not obvious slice to slice become much more so when fully rendered, leading to a smoother and more homogenous image.

References:

Chakeres, D., Whitaker, C., Dashner, R., Scharre, D., Beversdorf, D., Raychaudhury, A., Schmalbrock, P. 2005. High-resolution 8 Tesla imaging of the formalin-fixed normal human hippocampus. Clinical anatomy 18:88-91.

Duvernoy, H.M., 2005. The human hippocampus. Functional anatomy, vascularization and serial sections with MRI, Third edition. Springer. Verglag, Berlin.

Fatterpekar, G., Naidich, T., Delman, B., Aguinaldo, J., Gultekin, S., Sherwood, C., Hof, P., Drayer, B., Fayad, Z. 2002. Cytoarchitecture of the human cerebral cortex: MR microscopy of excised specimens at 9.4 Tesle. AJNR Am J Neuroradiol 23:1313-1321.

Mai, J. K., Assheuer, J., Paxinos, G. 2004. Atlas of the human brain. Elsevier. San Diego, California.

Mueller, S.G., Stables, L., Du, A.T., Schuff, N., Truran, D., Cashdollar, N., Weiner, M. W., 2007. Measurements of hippocampal subfields and age related changes with high resolution MRI at 4T. Neurobiol Aging 28(5):719-726.

Thammaroj, J., Santosh, C., and Bhattacharya, J. 2005. The hippocampus: modern imaging of its anatomy and pathology. Practical Neurology.

Yushkevich, P., Avants, B., Pluta, J., Das, S., Minkoff, D., Mechanic-Hamilton, D., Glynn, S., Pickup, S., Liu, W., Gee, J., Grossman, M., & Detre, J. 2009. A high-resolution computational atlas of the human hippocampus from postmortem magnetic resonance imaging at 9.4T. NeuroImage 44:385-398.

Zhan, J., Brys, M., Glodzik, L., Tsui, W., Javier, E., Wegiel, J., Kuchna, I., Pirraglia, E., Li, Y., Mosconti, L., Saint Louis, L., Switalski, R., De Santi, S., Kim, B., Wisniewski, T., Reisberg, B., Bobinski, M., and de Leon, M. 2009. An entorhinal cortex sulcal pattern is associated with Alzheimer's disease. Human Brain Mapping 30:874-882.